NASA/TM-20240005040

X-57 Maxwell High Lift Motor Controller Electromagnetic Interference Test Results

Michael J. Garrett, Susanah R. Kowalewski, and Matthew G. Granger
Glenn Research Center, Cleveland, Ohio

July 2024

NASA STI Program Report Series

NASA/TM-20240005040

X-57 Maxwell High Lift Motor Controller Electromagnetic Interference Test Results

Michael J. Garrett, Susanah R. Kowalewski, and Matthew G. Granger
Glenn Research Center, Cleveland, Ohio

National Aeronautics and
Space Administration

Glenn Research Center
Cleveland, Ohio 44135

July 2024

This work was sponsored by the Integrated Aviation Systems Program at the NASA Glenn Research Center.

Level of Review: This material has been technically reviewed by technical management.

This report is available in electronic form at https://www.sti.nasa.gov/ and https://ntrs.nasa.gov/

NASA STI Program/Mail Stop 050
NASA Langley Research Center
Hampton, VA 23681-2199

X-57 Maxwell High Lift Motor Controller Electromagnetic Interference Test Results

Michael J. Garrett, Susanah R. Kowalewski, and Matthew G. Granger
National Aeronautics and Space Administration
Glenn Research Center
Cleveland, Ohio 44135

Summary

During research and development for NASA's X-57 Maxwell all-electric aircraft project, the efficiency and power density requirements of its electric propulsion subsystem components were met, but aspects of integrating its powertrain subsystems proved problematic. Electromagnetic interference (EMI) from the cruise motor controller (CMC) was a significant challenge for the project. This problem was exacerbated by the lack of EMI requirements imposed on subsystem powertrain components. This report presents the results of EMI testing of the X-57 high lift motor controller (HLMC) at the NASA Glenn Research Center's EMI Laboratory. For reference, the conducted emissions are compared to DO–160G and MIL–STD–61G conducted emissions limits. After the EMI test, mitigation of the conducted emissions using lightweight EMI chokes produced at NASA Glenn was evaluated using the Fast Fourier Transform (FFT) capability of an oscilloscope in the hardware development laboratory. This process can contribute to the rapid prototyping of electric powertrain components and EMI filters and improve the likelihood of successful EMI qualification at the component and system levels.

Nomenclature

AC	alternating current
CE102	Conducted emissions requirement in the MIL–STD–461 test standard
CMC	cruise motor controller
DC	direct current
DEP	distributed electric propulsion
dv/dt	voltage derivative over time
EMC	electromagnetic compatibility
EMI	electromagnetic interference
FFT	Fast Fourier Transform
HLMC	high lift motor controller
HVDC	high-voltage direct current
LISN	line impedance stabilization network
LRU	line replaceable unit
LVDC	low-voltage direct current
RF	radio frequency
SiC	silicon carbide

Introduction

NASA's X-57 Maxwell was an aircraft testbed designed to run exclusively on battery-sourced electrical power for propulsion and avionics. The project was part of NASA's investment to drive efficient and sustainable aviation. As an aircraft testbed, the X-57 aircraft powertrain included a cruise motor propulsion system responsible for steady-state propulsion at altitude and a distributed electric propulsion (DEP) system for added thrust at takeoff and altitude transitions. In the baselined propulsion system design, a 65-kW cruise motor was integrated into each wing; these motors were controlled and powered by two cruise motor controllers (CMCs). Additionally, a DEP system was to be integrated; six 14-kW high lift electric motors were integrated on each wing, with each motor powered and controlled by a single high lift motor controller (HLMC). During the final years of the X-57 project, the DEP system was descoped to allow focusing on the CMC design, development, and testing. Before the high lift system was descoped, the HLMC development tests demonstrated that highly efficient power processing can be achieved at high power density with wide bandgap silicon carbide (SiC) switches. In the altitude wind tunnel qualification test, the HLMC achieved greater than 97 percent efficiency at 11 kW with a mass of 1 kg (Ref. 1). The design and performance was improved to 14 kW after the altitude qualification (Ref. 2).

Electromagnetic Interference on X-57

The X-57 project continued with development of the cruise motor system but encountered several challenges. One of the most significant challenges occurred during integrated testing, when the high voltage derivative over time (dv/dt) of the CMC inverter switches generated common-mode currents that coupled over the power bus leads and through parasitic capacitances to low-voltage avionics systems, causing them to malfunction (Ref. 3). One lesson learned from the X-57 project was the necessity for electromagnetic interference (EMI) and electromagnetic compatibility (EMC) design, analysis, and/or testing at each assembly level (Ref. 4). Requirements and mitigation approaches for EMC must be developed for the printed circuit board assembly level, component, or line replaceable unit (LRU) level, subsystem level, and integrated system level for complex electrical systems, which includes aircraft with highly efficient submegawatt and megawatt powertrains (Ref. 5).

Significant effort was expended in troubleshooting EMI issues on the X-57. However, this report is the first publication of emissions measurements in an EMI laboratory. Limited EMI testing of a development unit HLMC at the EMI Laboratory at NASA Glenn Research Center was completed using test methods specified in RTCA DO–160G (Ref. 6) and MIL–STD–461G (Ref. 7). Conducted current emissions results were compared to Category H limits of DO–160, Section 21. Category H includes aircraft locations that may be in view of receivers (i.e., outside of the fuselage), which would be appropriate for the motor controllers in the aircraft wing nacelles. Conducted voltage emissions were measured according to the CE102 method from MIL–STD–461G.

HLMC EMI Test Method and Setup

The HLMC was set up in NASA Glenn’s EMI Laboratory semi-anechoic shield room for the EMI test in accordance with DO–160G, Sections 20 and 21, as shown in Figure 1. The HLMC was mounted to a cold plate assembly to accommodate cooling by connected fluid hoses in the place of having a nacelle cooled by airflow from a motor and propellor. The cold plate was bonded to the ground plane, but the high-voltage direct current (HVDC) leads were isolated from ground except at the HVDC power supply, in accordance with the X-57’s grounding design. The 13.8-Vdc, low-voltage direct current (LVDC) avionics bus return was grounded. Power to the HVDC and LVDC buses was supplied through line impedance stabilization networks (LISNs) in accordance with DO–160G.

Each output phase of the HLMC was loaded with a 0.24-mH inductor in series with the resistance of a three-phase resistive load bank. The load bank’s resistance was preset to a 14-kW load to the HLMC. The HVDC bus power was provided by a 500-Vdc power supply. A fluid recirculator supplied cooling water to the HLMC cold plate. As shown in Figure 2, the load inductors, resistive load bank, HVDC power supply, and chiller were set up in the adjacent reflective chamber of the EMI Laboratory. All interconnections passed through a pipe feedthrough to the semi-anechoic chamber with the exception of the HVDC power leads, which were routed through a high-voltage, low-pass filter between the semi-anechoic and reflective chambers. The control computer, also in the reflective chamber, was connected to the HLMC through a fiber optic link, as designed for the integrated HLMC on X-57.

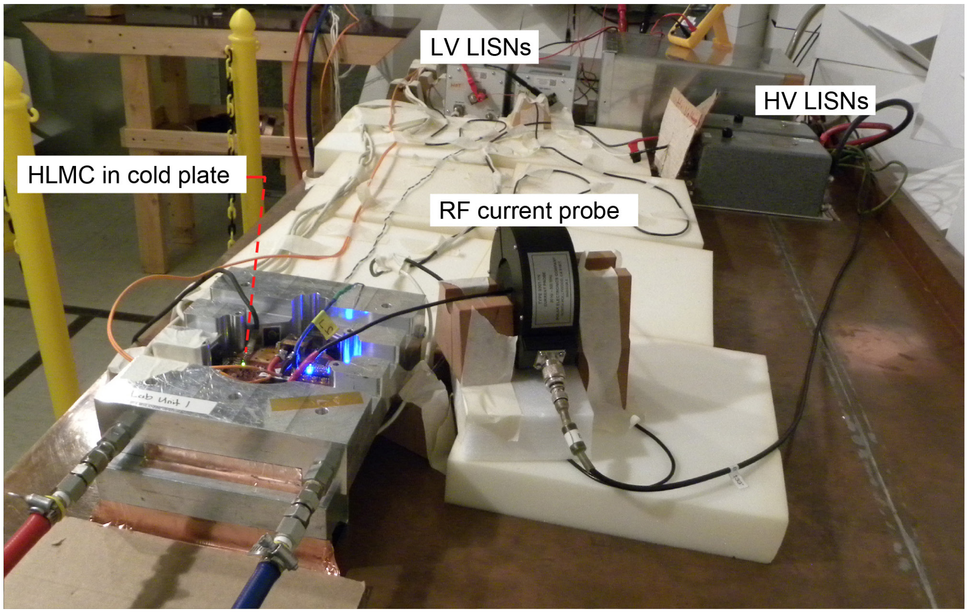

Figure 1.—HLMC EMI test setup in NASA Glenn's semi-anechoic EMI chamber.

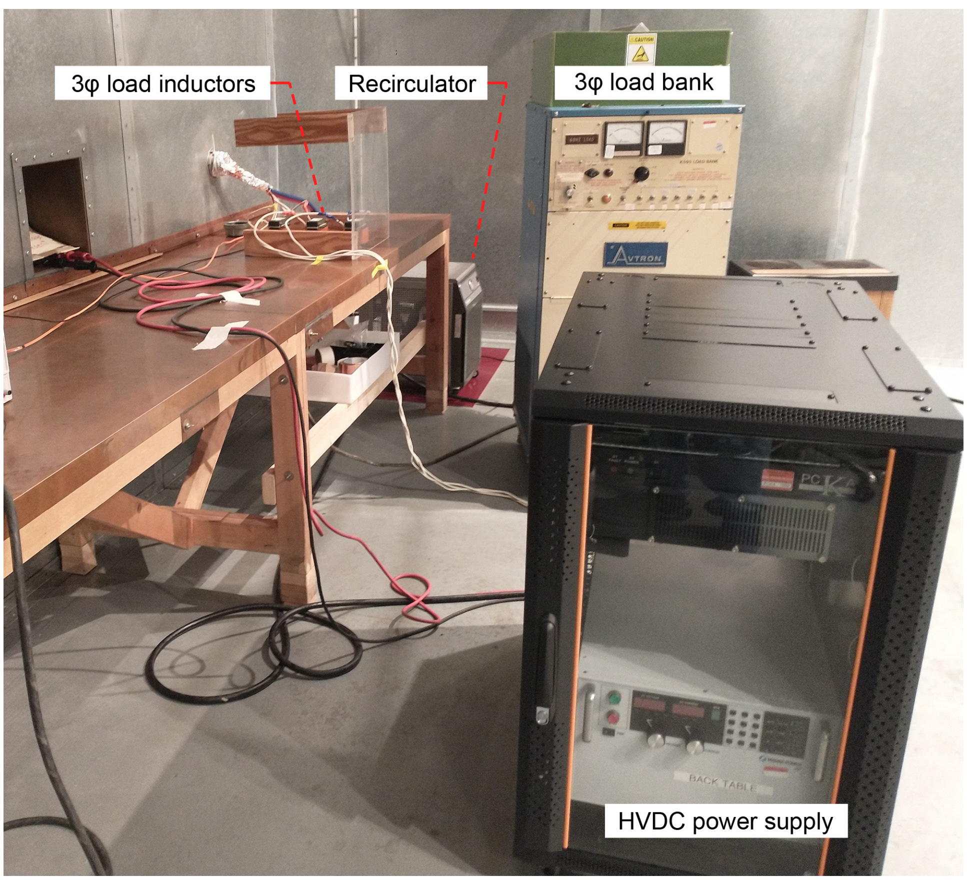

Figure 2.—X-57 HLMC test support equipment in adjacent reflective chamber.

EMI Test Results

The results of the radio frequency (RF) conducted emissions tests of the HLMC are presented in this section. While reviewing these results, it is important to note that neither the HLMC nor the integrated X-57 aircraft were required to meet the requirements of DO–160G. The emissions limits mentioned with each measurement are provided for reference. Also, note that for each test configuration, noise floor measurements with the HLMC unpowered but with all test support equipment powered, were 15 dB or more lower than the respective limit. Figure 3 shows the RF conducted current emissions on the HVDC hot lead, with the HLMC operating at 14-kW output. The amplitude of the harmonics of the switching are as high as 92 dBμA (~40 mA_{RMS}) and are clearly higher than the DO–160G, Section 21.4, Category H, power lead limit. However, given that DO–160G does not address direct current (DC) power buses higher than 270 Vdc, the limit shown would not have applied to the X-57 traction bus and is shown only for reference.

The CE102 RF conducted emissions test in the MIL–STD–461G standard evaluates the conducted RF voltage emissions of the equipment under test on DC bus leads. The appendix of the standard explains that the CE102 limit is chosen to provide margin below the MIL–STD–704's allowed distortion spectrum in that power-quality standard. Therefore, the CE102 measurement would be most relevant if the HLMC is on a shared bus with other loads. Figure 4 plots the RF voltage emissions from the 500-Vdc hot lead of the HLMC with a 14-kW load. In this figure, the limit has been raised by 12 dB in accordance with the CE102 test procedure for voltages higher than 440 Vdc. Like the hot lead current spectrum, the switching harmonics dominate the voltage spectrum. Because CE102 starts at 10 kHz, emissions at the fundamental frequency at 39.5 kHz are evident. Maximum levels of the HVDC hot lead voltage spectrum reach 123 dBμV (1.4 V_{RMS}) at 500 kHz.

Given the hot lead emissions of the HLMC, a differential-mode filter would likely be required if emissions limits were levied on the HLMC to protect other avionics equipment on the HVDC bus. However, electric aircraft developers may consider developing their components for use on private HVDC buses dedicated exclusively to the motor controller. With this approach, the differential filter design for an HVDC bus would not be driven by power-quality requirements levied on a shared DC bus.

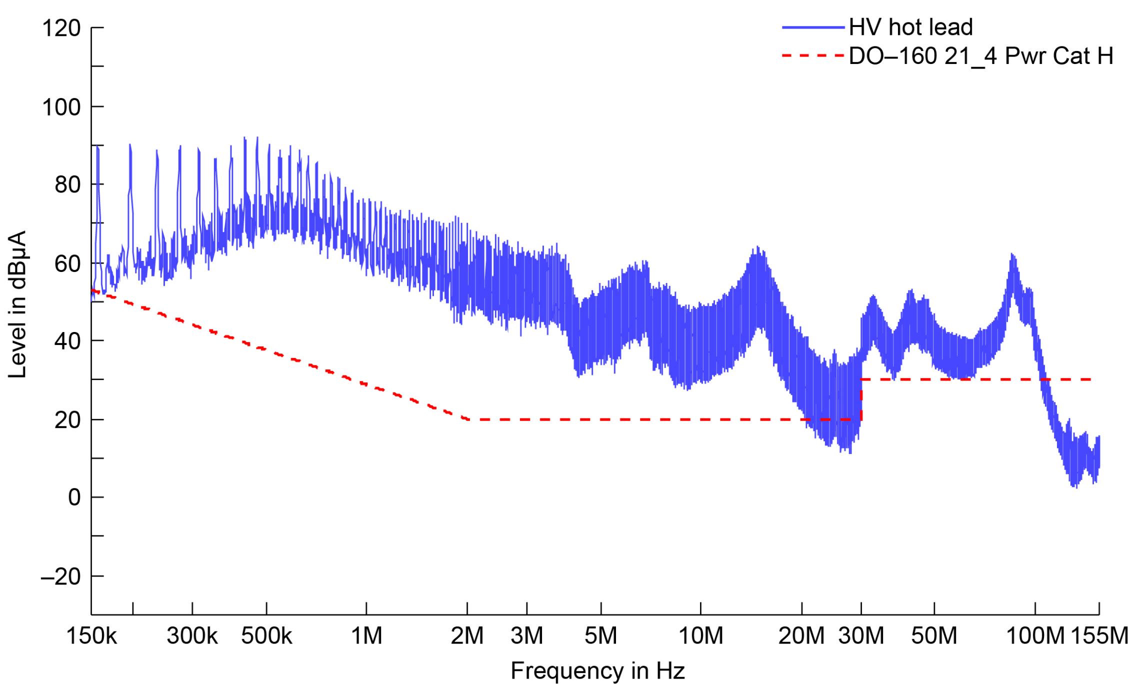

Figure 3.—HLMC 500-Vdc hot lead DO–160G, Section 21, RF current emissions, 14-kW load.

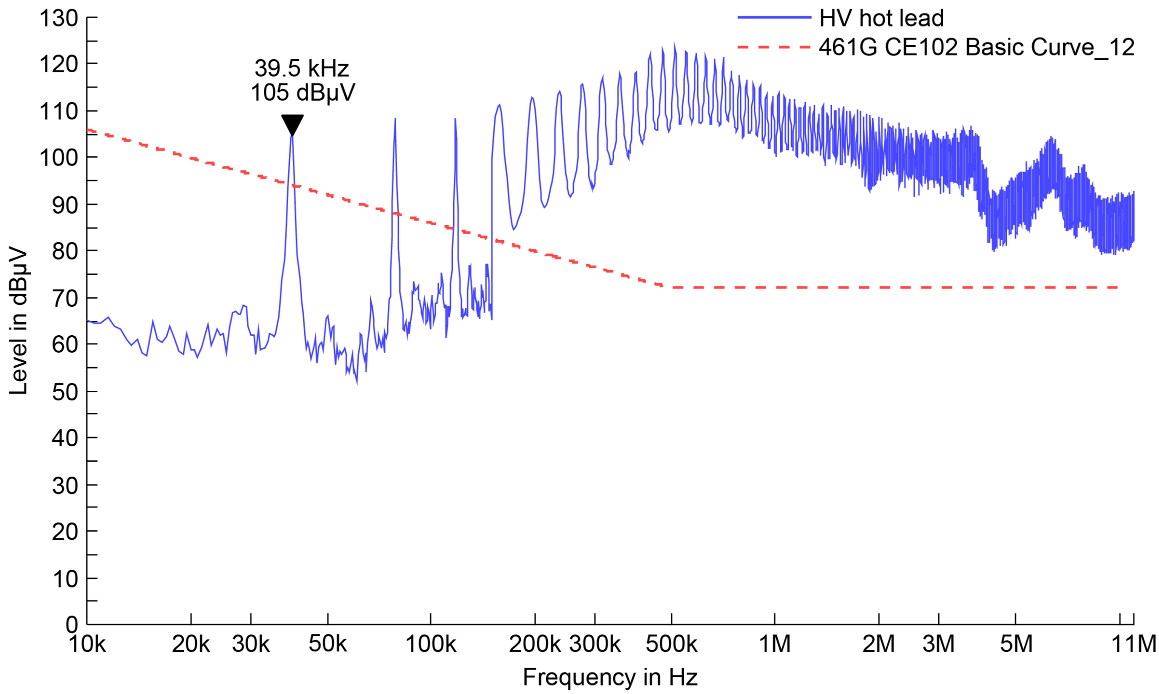

Figure 4.—HLMC 500-Vdc hot lead 461G CE102 RF voltage emissions, 14-kW load.

DO–160G, Section 21, also specifies conducted RF emissions measurements of interconnecting cable bundles, which are called bulk cable measurements. Note that primary power cables are exempt from the bulk cable measurement requirement by DO–160G, Section 21. However, measurement of bulk cable currents on power lines is commonly recommended to measure common-mode currents generated from switching power sources to assess the effectiveness of common-mode filtering. Also, common-mode currents are a predictor of radiated emissions (Ref. 8). The bulk cable emissions of all HLMC cables are plotted in Figure 5. Once again, the harmonics of the 40-kHz switching frequency dominate, with the highest levels across the spectrum coming from either the 500-Vdc input cable or the three-phase output cable. This makes sense because the leads of these cables are connected to the switching inverter. The arm cable carries a 13.8-Vdc logic state for the HLMC controller to control the enabling of the HLMC for operation through the user interface. Despite the near-DC bandwidth of the arm circuit signal and fiber optic isolation on the HLMC control board (Ref. 2), the arm cable current emissions exceed the emissions of the HVDC cable at several frequencies. At these frequencies, capacitive coupling from the HVDC cable and/or the alternating current (AC) output cable may be coupling onto the arm cable. The LVDC avionics bus cable’s conducted emissions are the lowest over most of the spectrum and are less than the Category H limit from 10 to 150 MHz. Nonetheless, given that the LVDC cable and the arm cables were to be connected to the X-57’s cockpit avionics on the aircraft, mitigations against these emissions would likely have been required to prevent noise coupling to cockpit avionics systems. The HLMC conducted RF emissions test results reinforce lessons learned on X-57 to implement component-level EMI requirements and testing (Refs. 3 to 5).

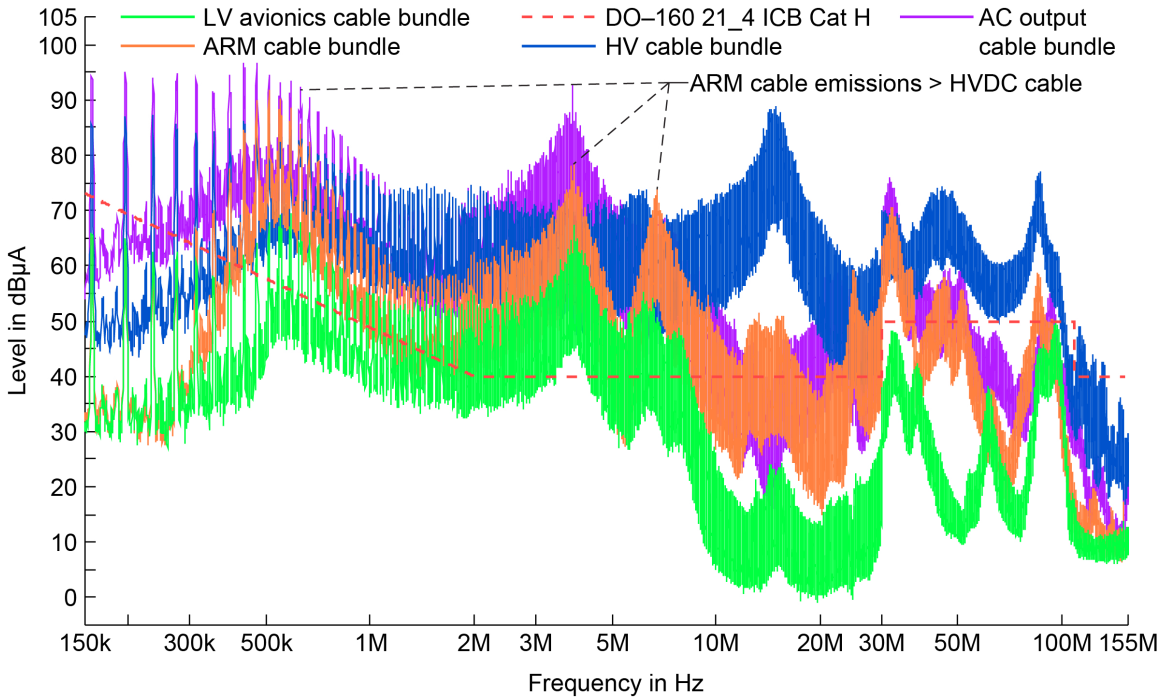

Figure 5.—HLMC DO–160G, Section 21.4, bulk cable RF current emissions, 14-kW load.

HLMC EMI Mitigation

Given that common-mode EMI challenges to the X-57 integration have been documented and that common-mode current is the major contributor to radiated emissions, NASA Glenn is developing lightweight, high-inductance, common-mode chokes to address this critical need for electrified aviation (Ref. 4). A custom-designed, 0.2-kg, 60-µH choke developed at NASA Glenn became available after the EMI test was performed. The lightweight choke was used in a common-mode LC filter and tested with the HLMC in the power electronics laboratory. Figure 6 illustrates the filter implementation.

The load for these tests was a liquid- and air-cooled electric motor driven at 4,000 rpm at an HVDC voltage of 500 Vdc. The motor loaded the HLMC to 2.5 kW. Figure 7 shows the filtered HLMC measurement setup.

A digital oscilloscope recorded the measurement data in the time domain; the emissions spectrum was generated using the scope's Fast Fourier Transform (FFT) function (Figure 8).

The oscilloscope was set to its maximum bandwidth of 200 MHz. Note that the DO–160 cable measurement bandwidths are specified at 1 kHz up to 30 MHz and 10 kHz from 30 MHz to 155 MHz, but the standard allows for wider measurement bandwidths, provided no correction factors are used for the wider bandwidths.

The measured spectral data from the oscilloscope required correction to account for the addition of an attenuator, which was used to protect the oscilloscope, and the current probe's frequency-dependent transducer factors. A custom MATLAB® (The MathWorks, Inc.) script was created to make this correction. Figure 9 is a plot of the HVDC bus bulk current spectrum without the filter, the spectrum with the LC filter, and the DO–160, Category H, limit line for bulk current measurements. As the wider bandwidth of the oscilloscope results in higher noise floors and likely higher emissions measurements, the spectrum plots are conservative with respect to the limit line. The filter provides 50 dB of attenuation from 100 kHz to 2 MHz and approximately 20 dB of attenuation to 150 MHz. The common-mode emissions are reduced below the limit except between 3 and 6 MHz, where an additional 15 to 20 dB of attenuation is required.

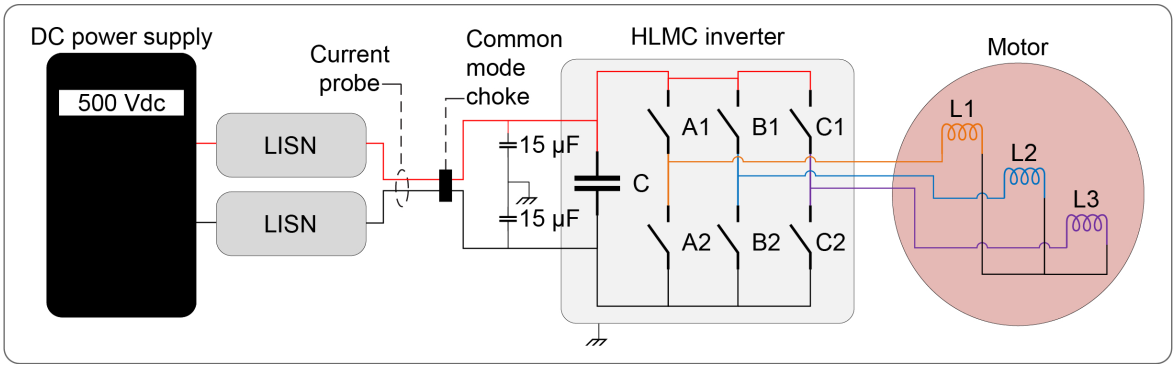

Figure 6.—HLMC test setup with LC common-mode filter.

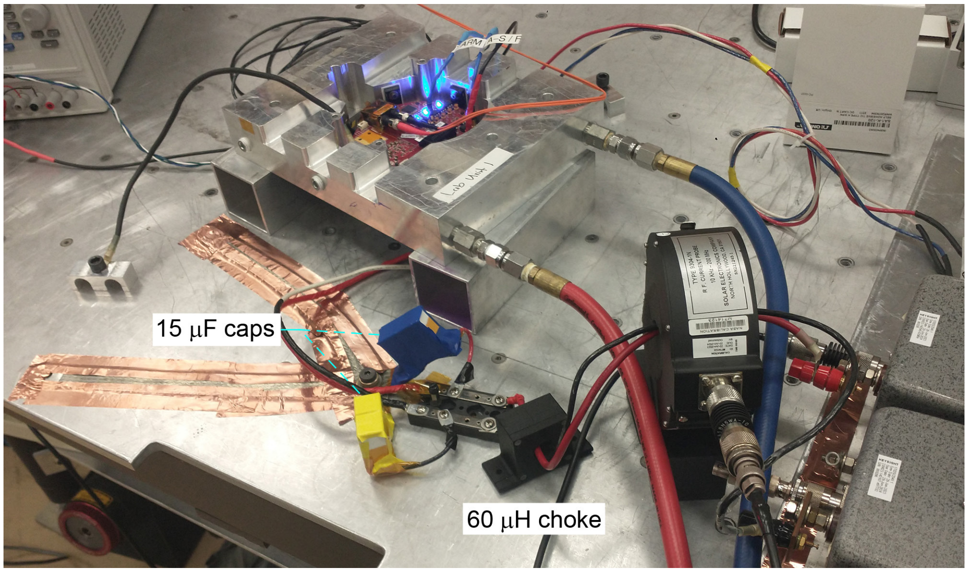

Figure 7.—HLMC with common-mode filter.

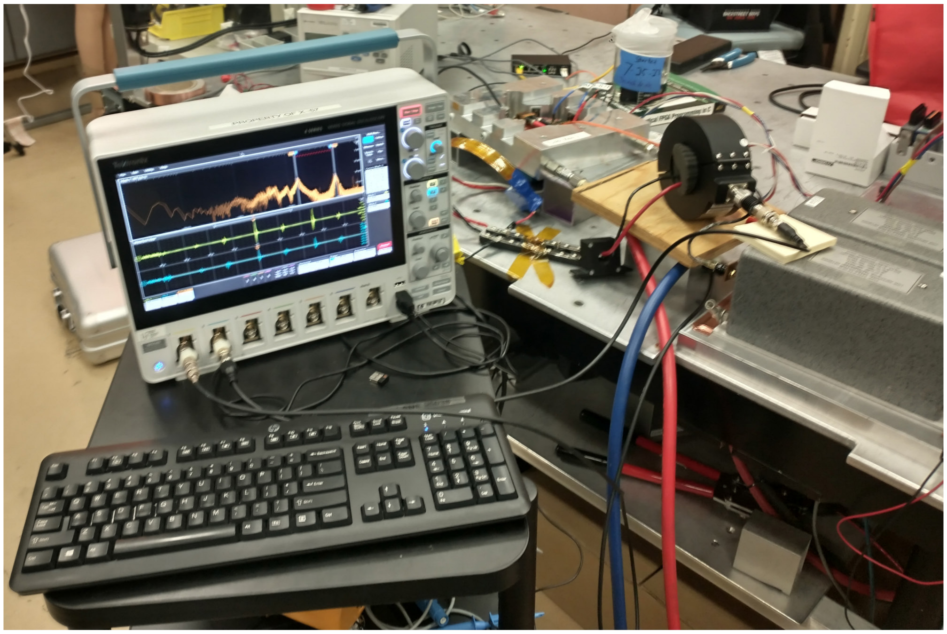
Figure 8.—EMI measurement with oscilloscope with FFT function.

Some leakage inductance is likely in the common-mode choke, which forms a differential-mode LC filter with the capacitor in each HVDC lead. The differential attenuation was evaluated by routing the HVDC leads so that DC flowed in the same direction through the current probe, canceling the common-mode contribution to the measurement (Figure 10). However, this lead configuration doubles the differential-mode current contribution to the measurement.

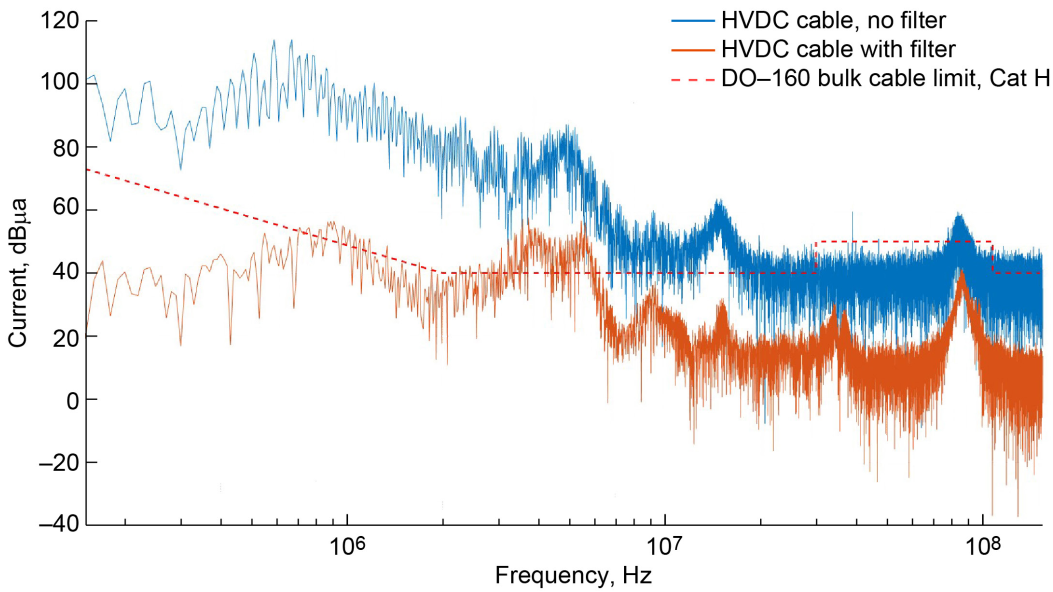

Figure 9.—HVDC bulk cable current filter attenuation, HVDC 500-V, 2.5-kW motor load.

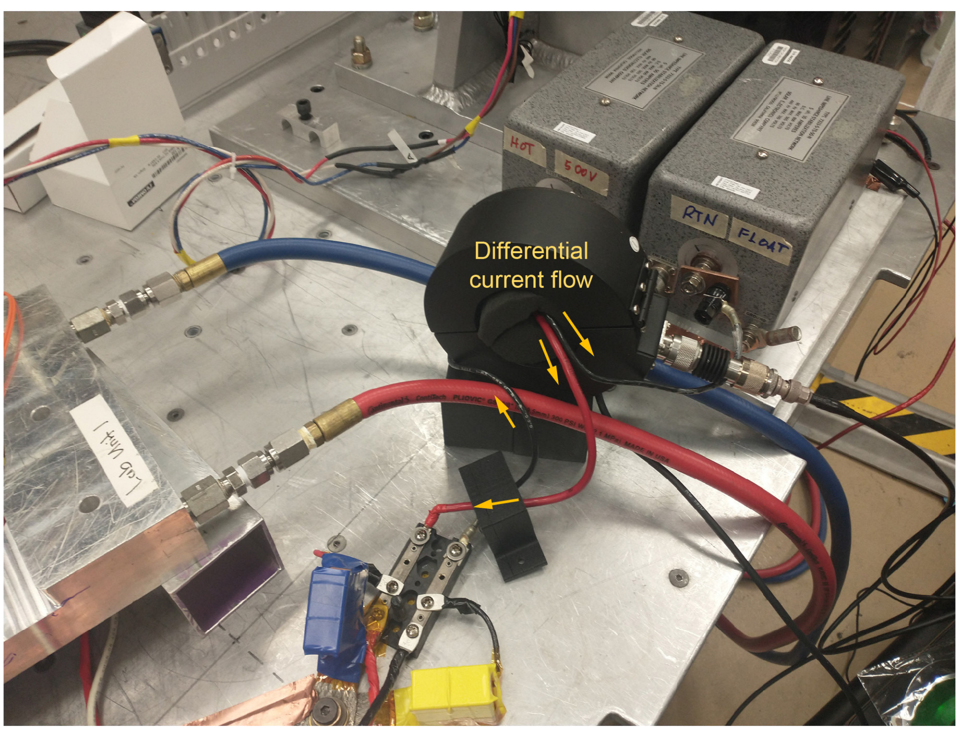

Figure 10.—HVDC bus differential current measurement setup with LC filter.

As shown in Figure 11, a modest 10 to 20 dB of differential current spectrum attenuation between 100 kHz and 1 MHz was achieved. A differential filter would be required with the common-mode filter to reduce the differential current noise on each lead over a larger portion of the spectrum.

The CE102 measurements plotted in Figure 12 show attenuation of from 10 to 30 dB between 100 kHz and 3 MHz. Here, the capacitors in the LC filter contribute significantly to the attenuation of the voltage spectrum.

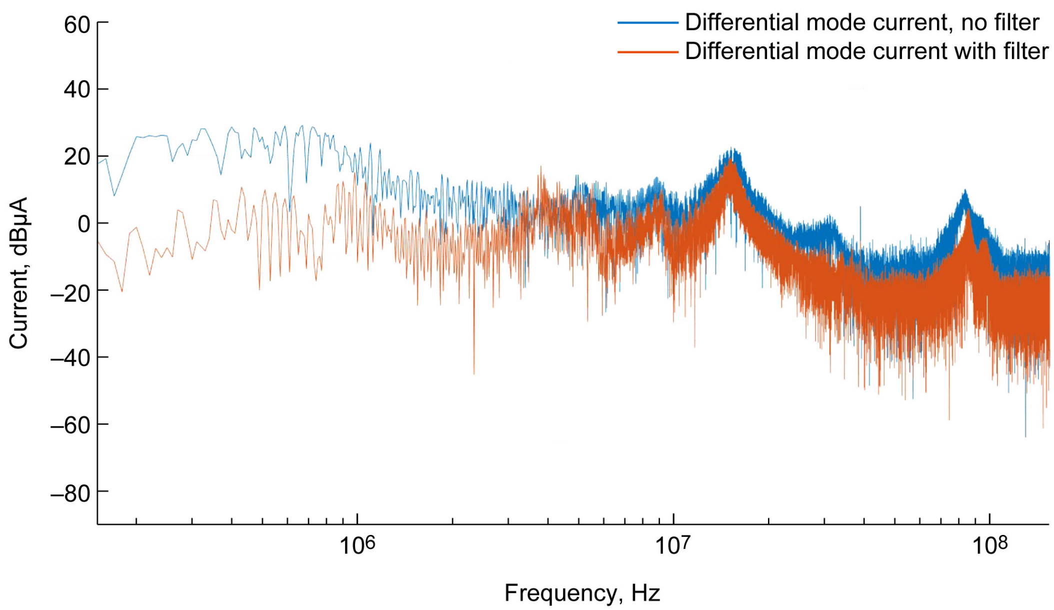

Figure 11.—HVDC bus differential current filter attenuation results, HVDC 500-V, 2.5-kW motor load.

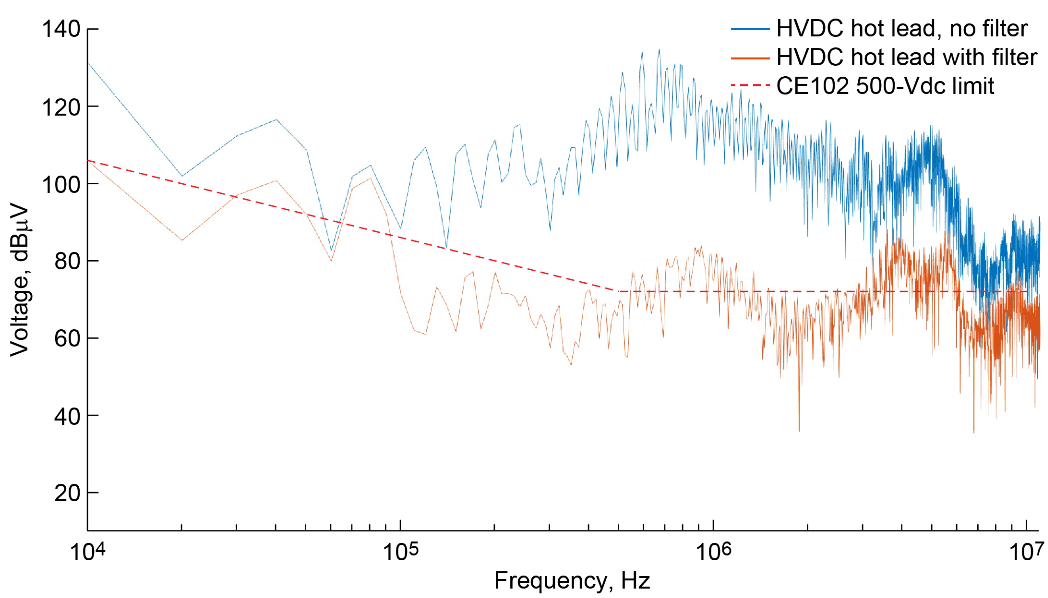

Figure 12.—HLMC DC hot lead, CE102 voltage measurement, HVDC 500-V, 2.5-kW motor load.

Conclusions

The electromagnetic interference (EMI) test results of the high lift motor controller confirm the lessons learned from X-57. To develop highly efficient powertrains, EMI mitigation and electromagnetic compatibility should be addressed at each level of development. System-level EMI requirements must be developed first, then component-level testing against requirements as determined by the integrator can confirm component-level design or reveal issues that can be solved at the component level with less effort and expense than at the level of the integrated system. Solutions may include reducing the EMI source function, like switching transients, reducing the coupling between the EMI source and receptor, like EMI filtering, or hardening potential receptors, like fiber optic transceivers, or any combination of these efforts. Conducted EMI measurements can be made quickly with a wide bandwidth current probe, line impedance stabilization networks, and an oscilloscope. This precompliance system can be used to quickly measure the effectiveness of EMI mitigations.

References

1. Garrett, Mike, et al.: Development of an 11 kW Lightweight, High Efficiency Motor Controller for NASA X–57 Distributed Electric Propulsion Using SiC MOSFET Switches. AIAA 2019–4400, 2019.
2. Kowalewski, S., et al.: NASA's X–57 High Lift Motor Controller: Detailed Design, Test Results, and Outcomes. AIAA Electric Aircraft Technologies Symposium, Las Vegas, NV, pending publication, 2024.
3. Clarke, Sean: X–57 Maxwell Aircraft EMI/EMC Integration Lessons Learned. Presented at the AIAA/IEEE Electric Aircraft Technologies Symposium, San Diego, CA, 2023.
4. Avanesian, David, et al.: X–57 Electromagnetic Interference Design, Integration, and Test Consideration. Presented at the AIAA/IEEE Electric Aircraft Technologies Symposium, San Diego, CA, 2023.
5. Perez, R.: Steps for the Proper Development of an EMC Control Plan. Proceedings of the 2002 IEEE International Symposium on Electromagnetic Compatibility, vol. 2, 2002, pp. 766–771.
6. Federal Aviation Administration: Environmental Conditions and Test Procedures for Airborne Equipment. RTCA DO–160, Version D, 2011.
7. Department of Defense: Requirements for the Control of Electromagnetic Interference Characteristics of Subsystems and Equipment. MIL–STD–461G, 2015.
8. Paul, C.R.: A Comparison of the Contributions of Common-Mode and Differential-Mode Currents in Radiated Emissions. IEEE Trans. Electromagn. Compat., vol. 31, no. 2, 1989, pp. 189–193.